Electronic Supplementary Material (ESI) for Journal of Materials Chemistry C.

Plasmonic Au@Ag-upconversion nanoparticle hybrids for NIR photodetection via an alternating self-assembly method

Guoqiang Fang[1], Yanan Ji[1*], Qi Xiao[1], Xinyao Dong[1], Jinlei Wu[1], Jixin Zou[2], Yizhuo Xu[3], Wen Xu[1], Bin Dong[1*]

[1] Key Laboratory of New Energy and Rare Earth Resource Utilization of State Ethnic Affairs Commission, Key Laboratory of Photosensitive Materials & Devices of Liaoning Province, School of Physics and Materials Engineering, Dalian Minzu University, 18 Liaohe West Road, Dalian 116600, P. R. China.

[2] The Institute of Forensic Science, Ministry of Public Security, Beijing 100000, China.

[3] Material Science and Engineering College, Northeast Forestry University, Harbin 150080, China.

[*]E-mail: Yanan Ji (jiyn@dlnu.edu.cn); Prof. Bin Dong (dong@dlnu.edu.cn)

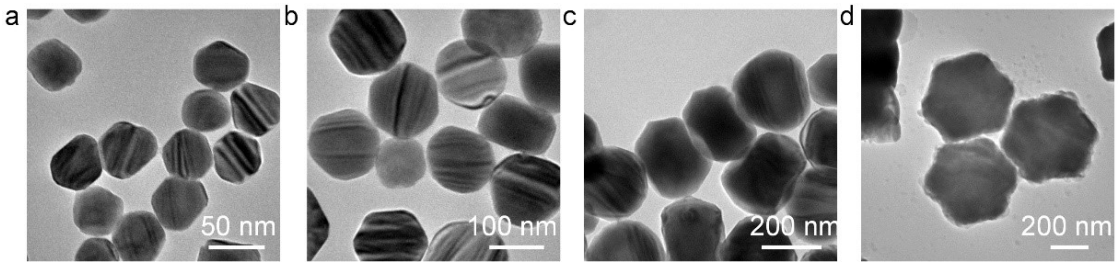

Figure S1. TEM images of 100, 150, 220, and 400 nm NaYF4: 20%Yb^{3+}, 2% Er^{3+} UCNPs.

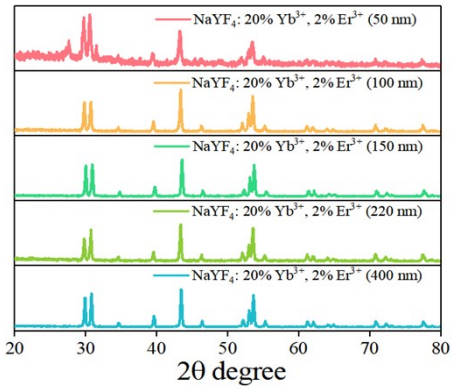

Figure S2. The XRD spectra of UCNRs with different sizes.

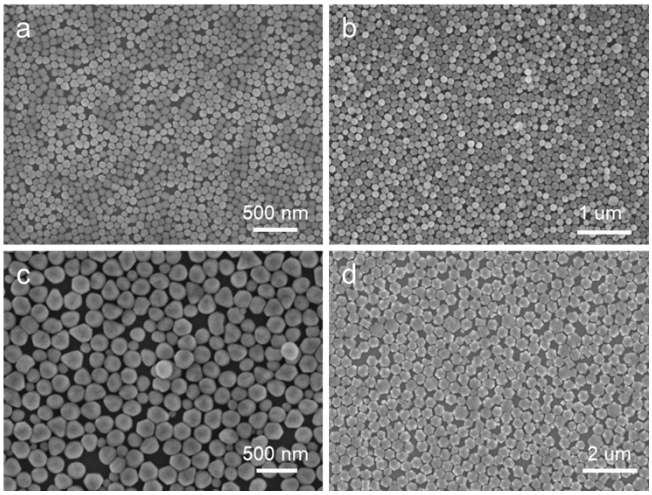

Figure S3. The SEM images of UCNPs monolayers of different sizes.

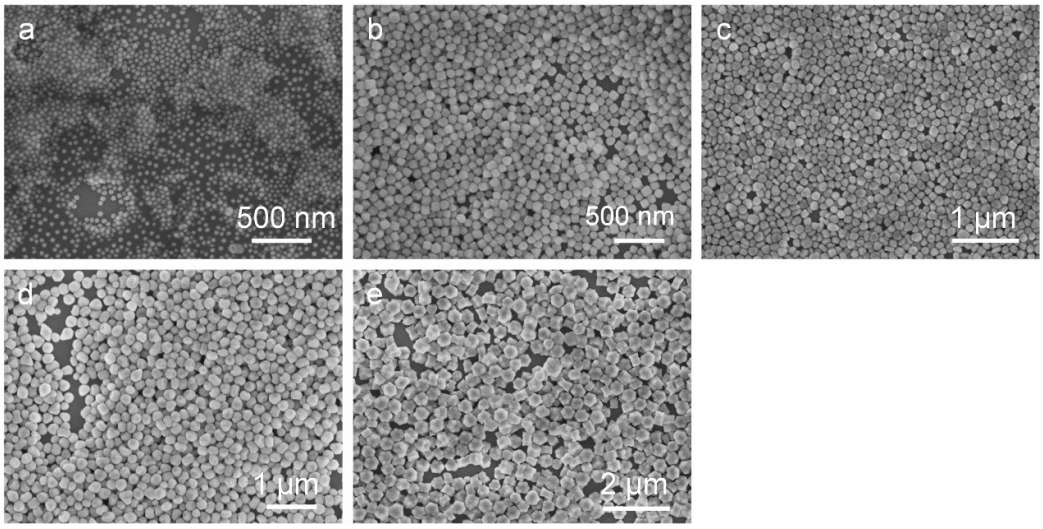

Figure S4. The different sizes of UCNPs samples film through spin-coating method. (a) 50 nm. (b) 100 nm. (c) 150 nm. (d) 220 nm. (e) 400 nm.

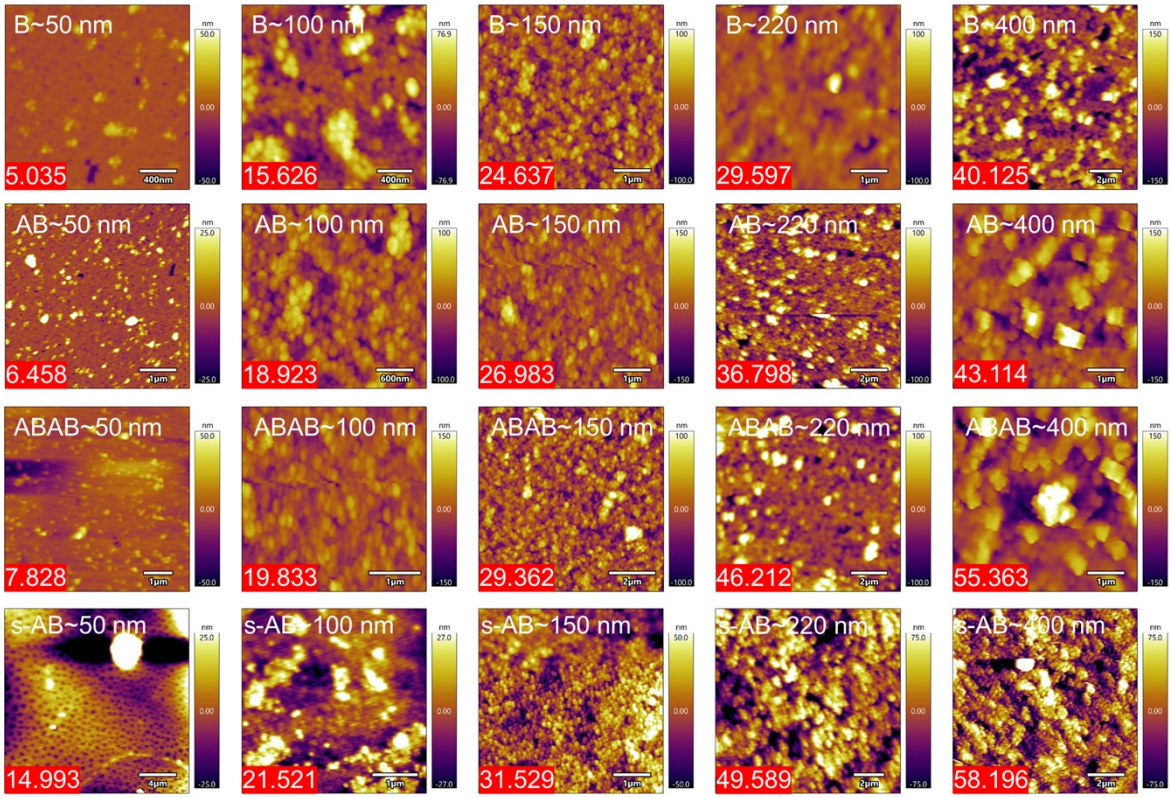

Figure S5. The surface roughness of B, AB, ABAB, and s-AB samples of five different diameters of UCNPs.

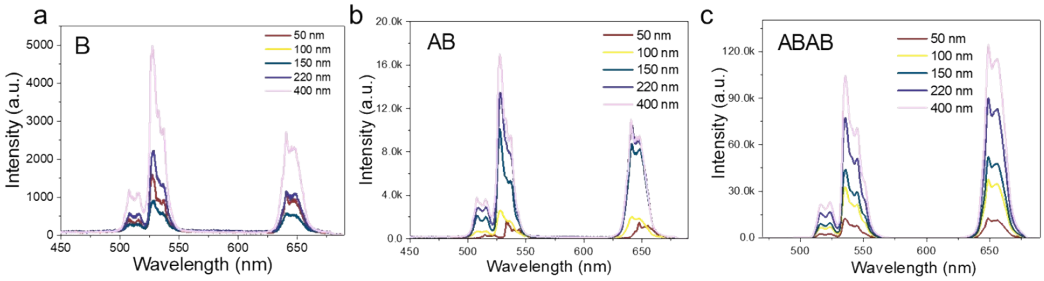

Figure S6. The typical upconversion emission of Er^{3+} ions under illumination at 980 nm of all sizes of (a) B samples, (b) AB samples, and (c) ABAB samples.

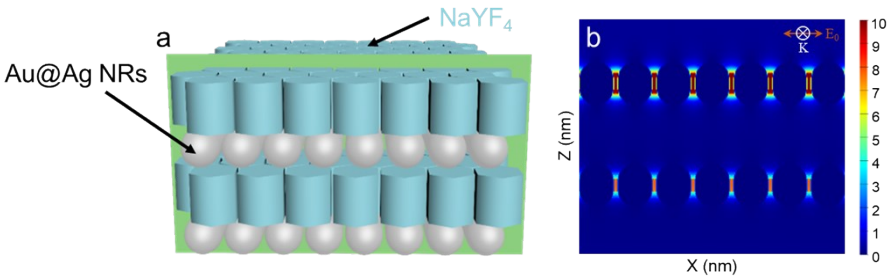

Figure S7. The electromagnetic field distribution xz planes for ABAB (50 nm) structure. (a) The electromagnetic field simulation model of xz plane in ABAB structure. (b) The electromagnetic field distribution in xz planes for Au@Ag NRs in ABAB structure. The plane (green) is at the center of the Ag NRs.

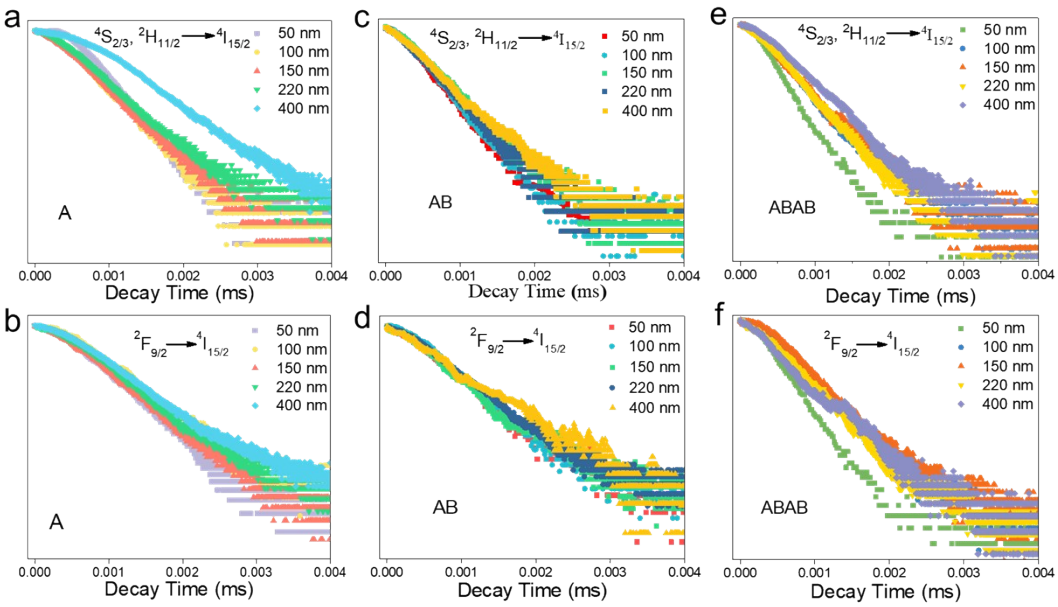

Figure S8. The luminescence dynamics of Er^{3+} emission at 980 nm excitation. (a), (b) A samples, (c), (d) AB samples and (e), (f) ABAB samples.

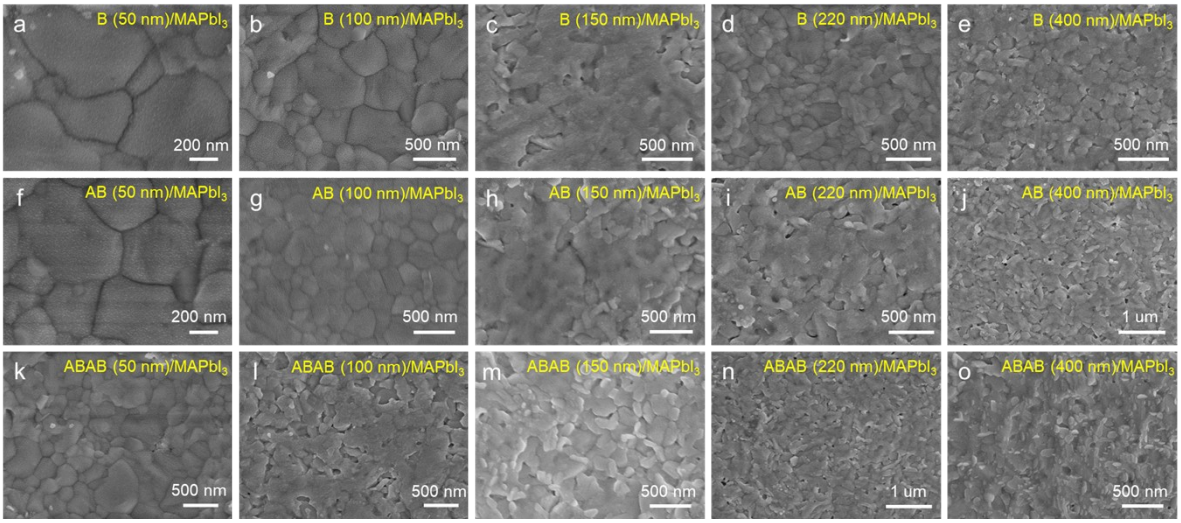

Figure S9. The top-view of SEM graphs of (a-e) B/$MAPbI_3$, (f-j) AB/$MAPbI_3$ and (k-o) ABAB/$MAPbI_3$.

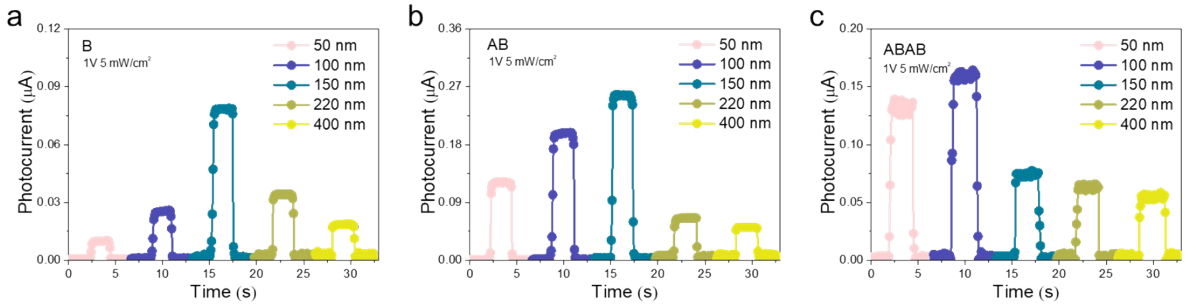

Figure S10. The on/off photocurrent-time (*I-t*) response curves of (a) B/$MAPbI_3$, (b) AB/$MAPbI_3$, (c) ABAB/$MAPbI_3$ PDs under the illumination of a 980 nm laser with intensity of 5 mW/cm^2 at the bias voltage of 1 V.

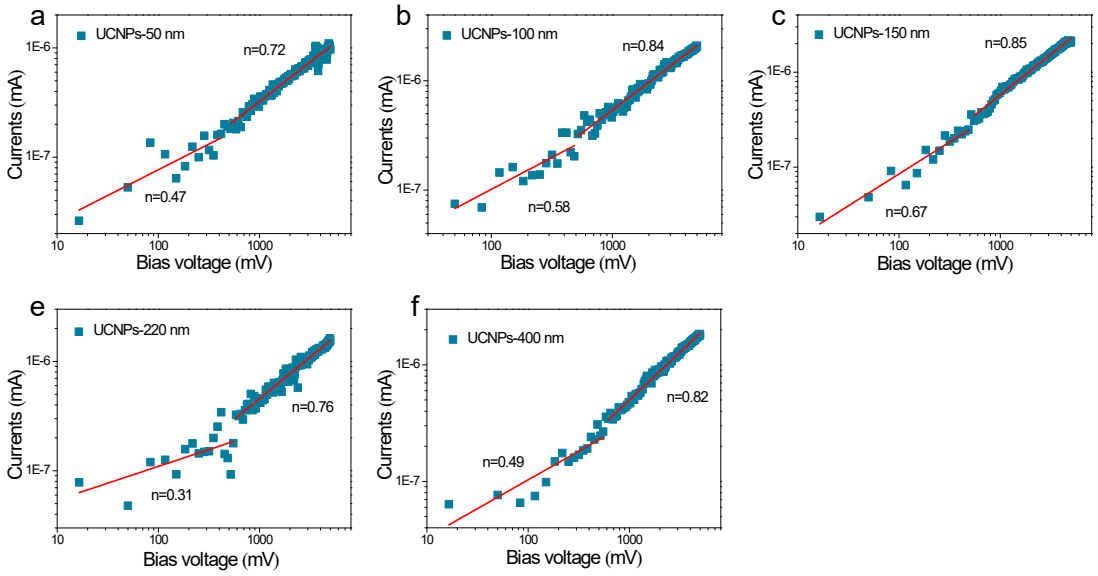

Figure S11. Dark *I-V* response of the $MaPbI_3$/UCNPs PDs, (a) B-50 nm. (b) B-100 nm. (c) B-150 nm. (d) B-220 nm. (e) B-400 nm.

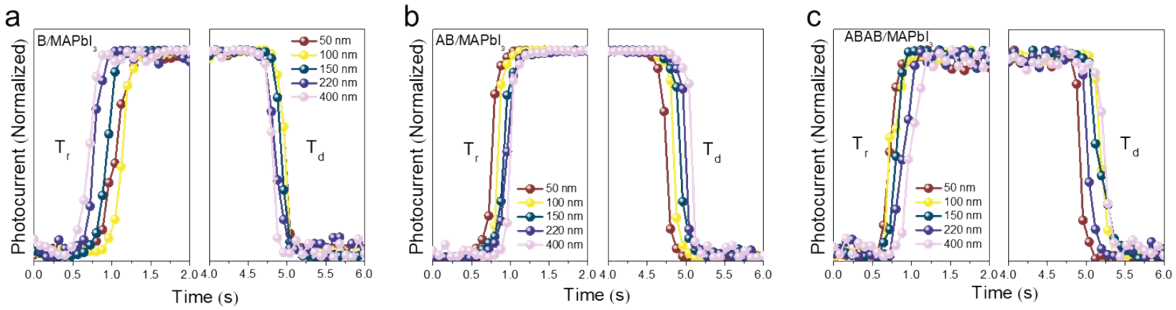

Figure S12. The exhibit rising (T_r) and decay (T_d) response time of (a) $B/MAPbI_3$, (b) $AB/MAPbI_3$ and (c) $ABAB/MAPbI_3$ PDs.

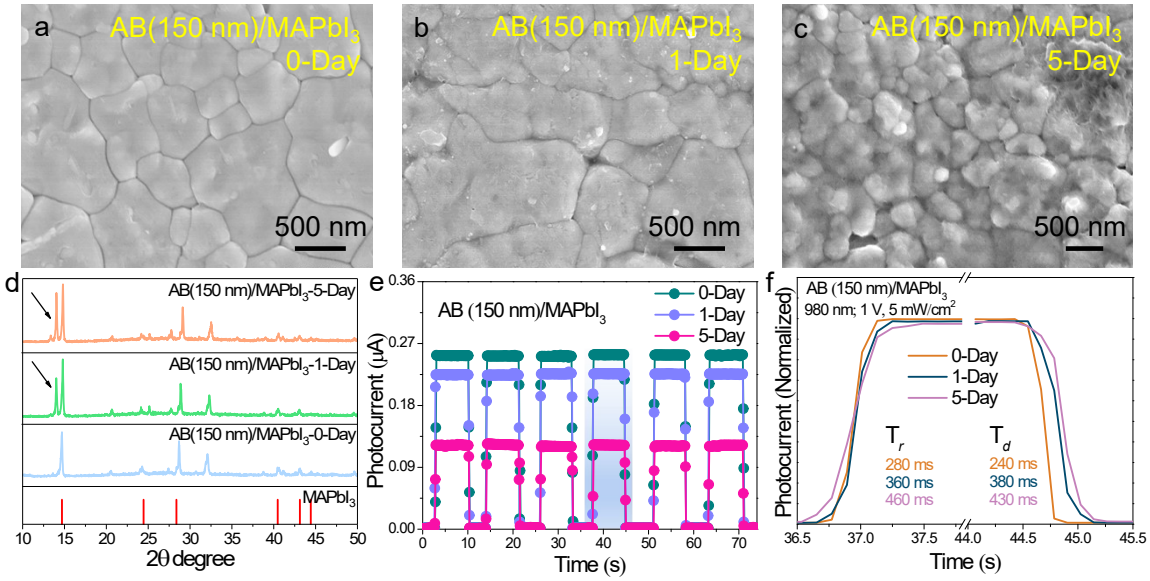

Figure S13. The influences of the moisture-induced degradation of perovskite layers on the device photocurrents. (a-c) Top-view of SEM image on the surface of the AB (150 nm)/$MAPbI_3$ PDs after 0-day (a), 1-day (b), and 5-day (c) of placement, respectively. The surface of the sample was slightly degraded after one day. While after 5 days, the surface degradation of $MAPbI_3$ layers were distinctly serious. (d) The in-situ X-ray diffraction pattern of AB (150 nm)/$MAPbI_3$ PDs under different conditions. The XRD spectrum of $MAPbI_3$ layer before almost no interaction with water vapor exhibits that the main component of the sample films is determined to be polycrystalline $MAPbI_3$. The peaks at the diffraction angles 14.07, 24.45, 28.37, 40.47, 43.12, and 44.42° are ascribed to the diffraction from the (110), (022), (220), (224), (141), and (134) planes of $MAPbI_3$, respectively.[1] After 1 day and 5 days, the characteristic peak of $MAPbI_3$ di-hydrate (black arrows) appeared obviously on the XRD spectrum. (e) The multi-cycle *I-t* response curves of AB (150 nm)/$MAPbI_3$ PDs after 0, 1, and 5 days of exposure to air (1 V, 5 mW/cm^2). After placing the device in the air for 1 day and 5 days, the photocurrents can be kept at 89% and 49% of the initial value (0 day), respectively. (f) The exhibit rising (T_r) and decay (T_d) response time of AB/$MAPbI_3$ PDs after 0-day, 1-day, and 5-day placement, respectively. Zooming in the *I-t* curves at the marked position in (e). The response of AB (150 nm)/$MAPbI_3$ PDs shows that the t_r are 280 ms, 360 ms, and 460 ms, t_d are 240 ms, 380 ms, and 430 ms after 0, 1, and 5 days, respectively. As the device is exposed to air for longer, its response to 980 nm laser gradually slows down.

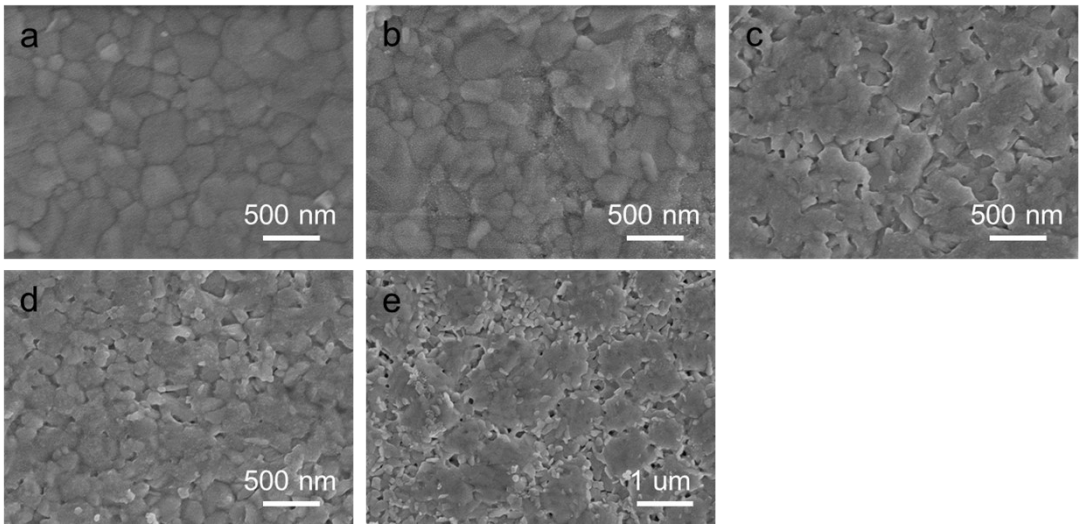

Figure S14. The top-view of the SEM images of s-AB/$MAPbI_3$ PDs. (a) B-50 nm. (b) B-100 nm. (c) B-150 nm. (d) B-220 nm. (e) B-400 nm.

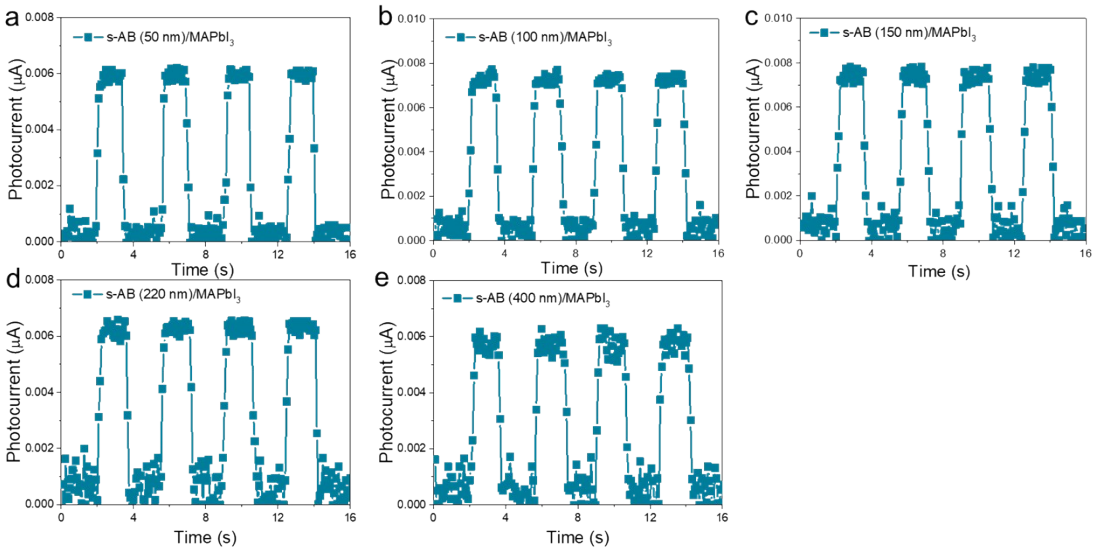

Figure S15. The *I-t* response curves of s-AB/$MAPbI_3$ under the illumination of a 980 nm laser with intensity of 5 mW/cm^2 at the bias voltage of 1 V. (a) B-50 nm. (b) B-100 nm. (c) B-150 nm. (d) B-220 nm. (e) B-400 nm.

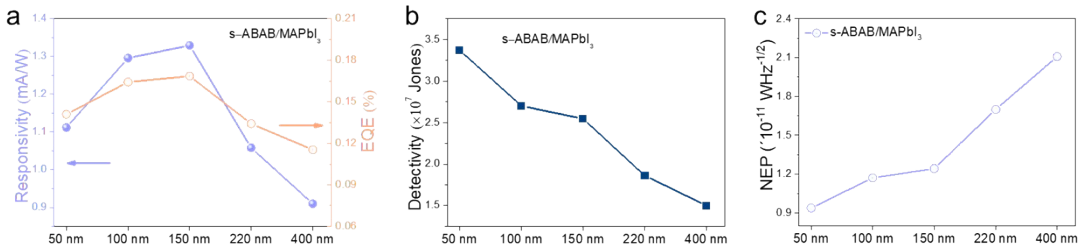

Figure S16. The (a) R (blue), D* (orange), (b) EQE and (c) NEP spectra of s-AB/ $MAPbI_3$ PDs.

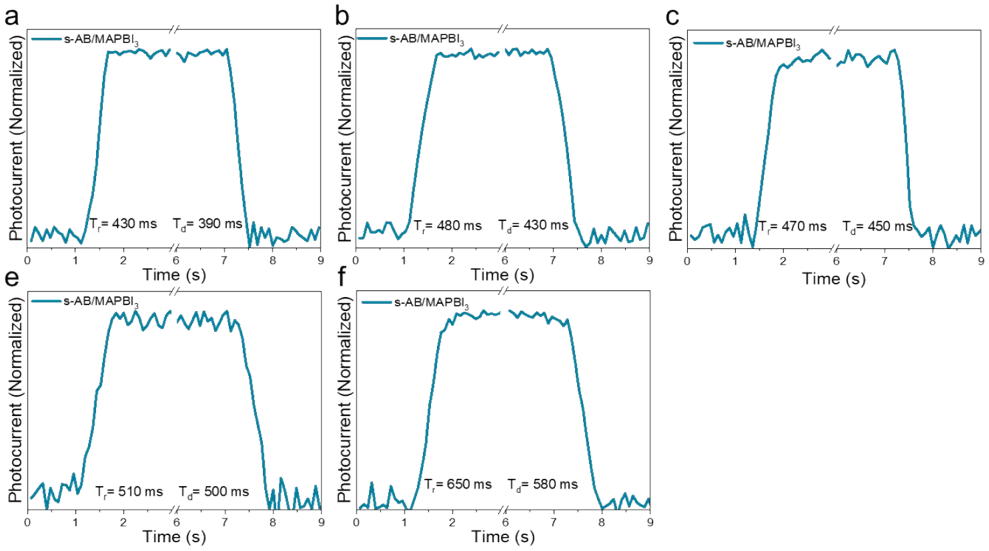

Figure S17. The exhibit rising (T_r) and decay (T_d) response time of s-AB/$MAPbI_3$. (a) B-50 nm. (b) B-100 nm. (c) B-150 nm. (d) B-220 nm. (e) B-400 nm.

References

1 M. Hada, Y. Hasegawa, R. Nagaoka, T. Miyake, U. Abdullaev, H. Ota, T. Nishikawa, Y. Yamashita and Y. Hayashi, *Japanese Journal of Applied Physics,* 2018**,** **57**, 028001.